Rapid Communications

# Millimetric granular craters from pulsed laser ablation

J. O. Marston[1] and F. Pacheco-Vázquez[2]
[1]*Department of Chemical Engineering, Texas Tech University, Lubbock, Texas 79409, USA*
[2]*Insituto de Fisica, Benemerita Universidad Autonoma de Puebla, Puebla 72570, Mexico*

(Received 15 January 2019; published 22 March 2019)

This Rapid Communication reports on an experimental study of granular craters formed by a mechanism, namely, optical energy, via a pulsed laser focused onto the surface of a granular bed. This represents an insight into granular cratering for two reasons; first, there is no physical contact between the initiation mechanism and the granular media (as typical for impact or explosion craters). Second, the resulting craters are millimetric in scale, which facilitates a test of energy scalings down to a previously unobserved lengthscale. Indeed, we observe a range of energy scalings conforming to $D_c \sim E^{\beta}$ with $\beta \approx 0.31$–$0.43$ depending on the characteristics of the granular media.

DOI: 10.1103/PhysRevE.99.030901

*Introduction*. Craters have been a curiosity of scientists for centuries [1–3] ever since Galileo first observed that the lunar surface is rough, and the observation of craters on the surface of the Earth and those on our nearby neighbors, i.e., the moon and mars, has been a key driver of sustained academic interest in both geophysics and planetary science. Today, it is well known that most of the craters observed on planetary surfaces were produced by impact of meteorites [1–3]. Other artificial mechanisms that also can produce craters include explosions [4–7] and the collapse of pressurized underground cavities [8]. However, of particular interest are the dark spots on Mars' polar ice caps and pits on Pluto, which are hypothesized to be granular materials ejected from below the ice, due to localized sublimation from solar radiation [9,10].

The existing literature on cratering is quite extensive and the two principal mechanisms, namely, impact cratering and explosive cratering, have been well established. However, in the latter case, systematic experiments at laboratory scale were only recently performed [11,12]. One consistent line of inquiry has been to derive the energy involved in the formation of a given crater and the mechanisms at play, which has led to many inverse problem studies [13–15], while other studies related to granular impact have focused on the penetration of the impacting projectile [16–23] and subsequent dynamics such as granular jets and ejecta curtains [24–26].

The general consensus is that the impact of projectiles yields near-parabolic craters, whose diameters, $D$, scale with energy [1–3,13–15], $E$, approximately as $D \sim E^{1/4}$. On the other hand, explosion craters are hyperbolic, nearly conical, whose diameter scaling is predicted [4–7] to follow a power law with energy, as $D \sim E^{1/3}$. Both of these power laws arise easily from dimensional analysis. However, in both cases, there are reported deviations from these laws. For impacts, significantly lower exponents were observed in the high-velocity regime [27–33], while in the case of explosive cratering, empirical evidence [4,7] indicates the exponent is actually 0.3. This discrepancy is partly explained by the confluence of ejecta fallback into the crater and material heterogeneity [7]. In fact, in the explosive regime, all scaling laws reported have been constrained between $1/4$ roots and $1/3$ roots of the explosive energy [4–7]. In a recent investigation [11], where a small mass of explosive (gunpowder mainly composed of potassium nitrate) was detonated in a sand bed, the resulting craters were best characterized by the power-law scaling $D \sim E^{0.3}$. In summary, while there is a wealth of literature on both impact and explosive cratering, there appear to be some unresolved issues, specifically pertaining to the scaling laws for explosive cratering, which have not yet been tested across multiple scales. This Rapid Communication aims to fill this knowledge gap by invoking a mechanism of cratering, namely, a pulsed laser system, only previously used for solid surfaces ablation [34–36], which enables the study of granular craters down to the millimetric scale.

*Experimental setup*. The principle component of the setup, shown in Fig. 1, consists of a pulsed laser (Quantel Utlra-50, Litron Nano-S), mirrors to guide the laser beam, and a focusing objective to concentrate the optical energy into a small focal spot ($\sim$100 $\mu$m). The laser beam is focused onto the surface of a granular bed contained in a small cylinder (width of 2 cm and depth of 1 cm) prepared from either silica glass beads with mean sizes $d = 31$, 149, or 178 $\mu$m or coarse sand with mean grain size of $d = 294$ $\mu$m, by pouring the media into the container and leveling with a straight-edged rule. The corresponding angles of repose, which quantify the internal friction, for the glass bead materials are $\theta_r = 35$, 24, and 30 (for $d = 31$, 149, and 178 $\mu$m) and $\theta_r = 34$ for the coarse sand.

The events were recorded with a high-speed video camera (Phatom V1611, Vision Research Ltd.) at frame rates up to 100 000 fps. Using a Nikon micro-Nikkor lens, we achieved a typical spatial resolution of 18 px/mm, i.e., approximately 55 $\mu$m/px. The laser pulse was triggered manually and an output Transistor-transistor logic signal simultaneously triggered the camera. The high-speed video sequences facilitated analysis of transient features, such as growth of the ejecta curtain, while high-resolution still photographs with a digital SLR camera (18 $\mu$m/px) enabled us to measure the final crater diameter, $D_c$, which could then be correlated to the laser energy.

 

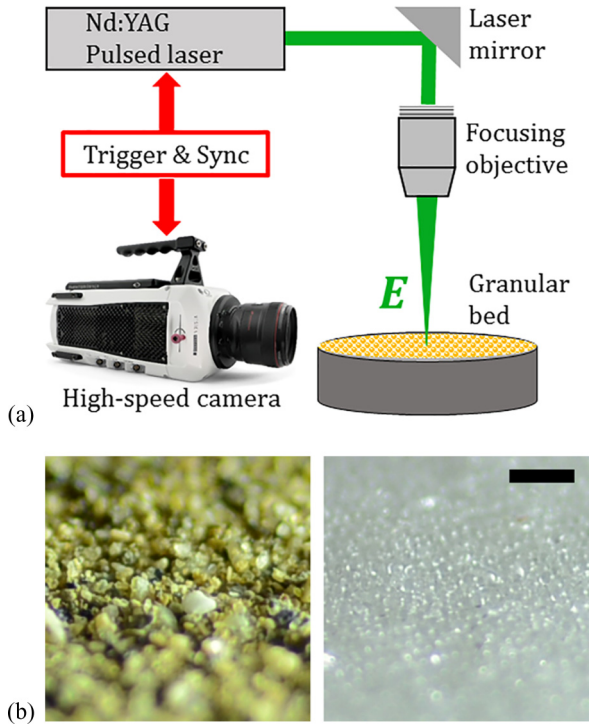


FIG. 1. (a) Schematic representation of the experimental setup used, showing the synchronized laser and high-speed imaging system, along with the optics used to direct and focus the laser pulse onto the granular bed. (b) Images of the granular surface for coarse sand (left) and glass beads (right) with 1 mm scale bar.

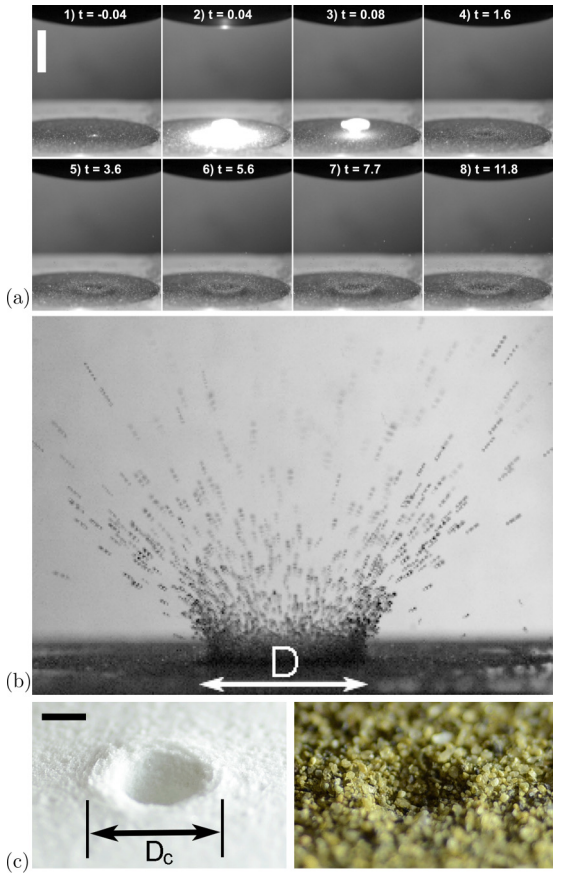


FIG. 2. (a) Image sequence showing the laser pulse and subsequent crater formation. The scale bar is 5 mm long and the images, relative to the trigger signal, are taken at $t = -0.04$, 0.04, 0.08, 1.6, 3.6, 5.6, 7.7, and 11.8 ms. (b) A five-frame streak image ($dt =$ 0.1 ms) showing particle tracks of individual grains and the curtain neck diameter, $D \approx 6$ mm. In both realizations, the laser pulse energy was 38 mJ and the grain size was 178 $\mu$m. (c) Examples of the final crater in fine glass beads $d = 31$ $\mu$m (left) and coarse sand (right) with 2 mm scale bar.

The input energy, $E$, of the event was selected by setting the Q-switch delay on the laser control panel from 290 $\mu$s down to 143 $\mu$s, which resulted in a range of energies $E \approx$ 1–38 mJ, as measured by a broadband optical energy meter. Several repeat trials were performed for each configuration.

*Laser pulse and crater formation*. Two representative videos are presented in image sequence format in Fig. 2, which show both (a) angled view and (b) true side-view perspectives, respectively. The former is used as an overview of the process, while the latter is a five-frame streak image from a side-view video showing the transient features such as grain trajectories and curtain neck diameter, $D(t)$. In Fig. 2(a) and hereafter, the time $t = 0$ corresponds to the precise moment that the laser pulse is triggered and seen in the frame. Due to the short pulse duration (8 ns) and small focal spot (~100 $\mu$m), the concentration of optical energy results in plasma formation due to rapid heating, indicated by the saturated region on the granular surface (bright spot in images 2 and 3). This energetic process imparts a localized pressure impulse around the focal spot and initiates the excavation process seen in images 4–8 of the sequence. The entire duration of the cavity formation depends upon the material and laser pulse energy, but is typically on the order of 10–100 ms.

At the conclusion of the excavation stage, the resulting crater appears reminiscient of those formed during impact and explosive cratering, with a raised rim around the periphery, as exemplified by Fig. 2(c). For clarity, we hereafter denote the transient ejecta curtain diameter as $D(t)$ and the final crater diameter as $D_c$.

*Energy scaling*. The ensemble raw data for crater diameter versus laser energy is presented in Fig. 3, showing the four different granular media and the full range of laser energies. Here, we observe that the craters are indeed all millimetric in diameter and increase monotonically with energy. For the glass beads, we observe that for any given energy, the crater diameter increases with the size of the beads. However, the coarse sand does not follow this trend, since the craters observed therein are smaller than even the finest glass beads. We postulate that this observation is due to a confluence of the wider relative size distribution, $\Delta S$, and the coarseness, $C$, of the grains themselves; The relative size distribution can be quantified by $\Delta S = (d_{90} - d_{10})/d_{50}$, taken from particle sizing (Malvern Mastersizer), while the coarseness can be given by circularity measurements as $C = 4A/P^2$, where $A$ and $P$ are the area and perimeter of two-dimensional grain profiles taken from microscope images. For the glass beads, $\Delta S < 1$ and $C > 0.9$, while for the coarse sand, $\Delta S > 1$ and $C < 0.8$. For the glass beads, we note that the relative size distributions are inversely related to the mean particle size with $\Delta S = 0.9$

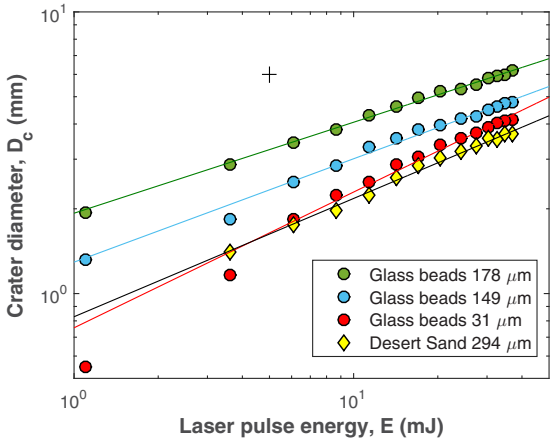


FIG. 3. Final crater diameter plotted as a function of the laser pulse energy for the four different granular media, indicated in the legend. The solid lines are the best power-law fits, $D_C \propto (E - E^*)^\beta$. A characteristic error bar is shown in the top left corner.

for $d = 31$ $\mu$m, and $\Delta S = 0.6$ for $d = 178$ $\mu$m. As such, rough particles are expected to give rise to a higher degree of particle "interlocking" [33,37]. In other words, coarseness and wider size distributions lead to higher internal friction in the granular bed resisting the propagation of energy imparted by the laser pulse, resulting in smaller craters.

The solid lines in Fig. 3 represent the best empirical fits with power-law models, $D_c = A(E - E^*)^\beta$, where the exponents are $\beta = 0.31$, 0.35, and 0.43 for glass beads with $d = 178$, 149, and 31 $\mu$m, respectively, while $\beta = 0.39$ for the coarse sand with $d = 294$ $\mu$m. The fitting parameter $E^* \sim O(10^{-1})$ mJ physically represents the critical energy required to form a crater with this technique, and is also used to form empirical relations for the temporal evolution of the ejecta curtain (see below). We note that $E^* \approx 0.3$ mJ for the larger glass beads, but $E^* \approx 0.8$ mJ for the finer glass beads and coarse sand, thus implying that both the magnitude of the pressure impulse *and* the friction of the bed are factored into this critical value.

At the laboratory scale, typical energies required for producing impact craters $D_c \sim O(10^{-2})$ m with dry grains $d \sim O(10^{-4})$ m are $O(10^{-4}$–$10^{-3})$ J [14,38,39], while those for explosions with $D_c \sim O(10^{-1}$–$10^{0})$ m are $O(10^{2})$ J[27]. However, In de Vet and de Bruyn [14], it was noted that the excavation energy, $E_x$, defined as the energy required to lift material out of the crater, was approximately 0.1%–0.5% of the impact energy for impact cratering, thus defining an effective "efficiency" of the cratering process. By approximating the crater shape with either a cone or hyperbola we can estimate the upper limit of the excavation energy $E_X \propto \rho_b \pi g D_C^4$, where $\rho_b$ is the bulk density of the bed. This yields values for $E_x$ on the order of $10^{-9}$–$10^{-7}$ J, whereas the laser pulse energy $E = O(10^{-3}$–$10^{-2})$ J. This implies significant energy loss which is expected to occur through three principal mechanisms, namely,- (i) kinetic energy of grains in the early ejecta curtain, (ii) friction due to interparticle collision, and (iii) thermal energy due to plasma formation. The first two are inherent in all cratering experiments, while the latter is unique to the pulsed laser initiation reported herein, and may constitute a significant proportion of the energy loss. In

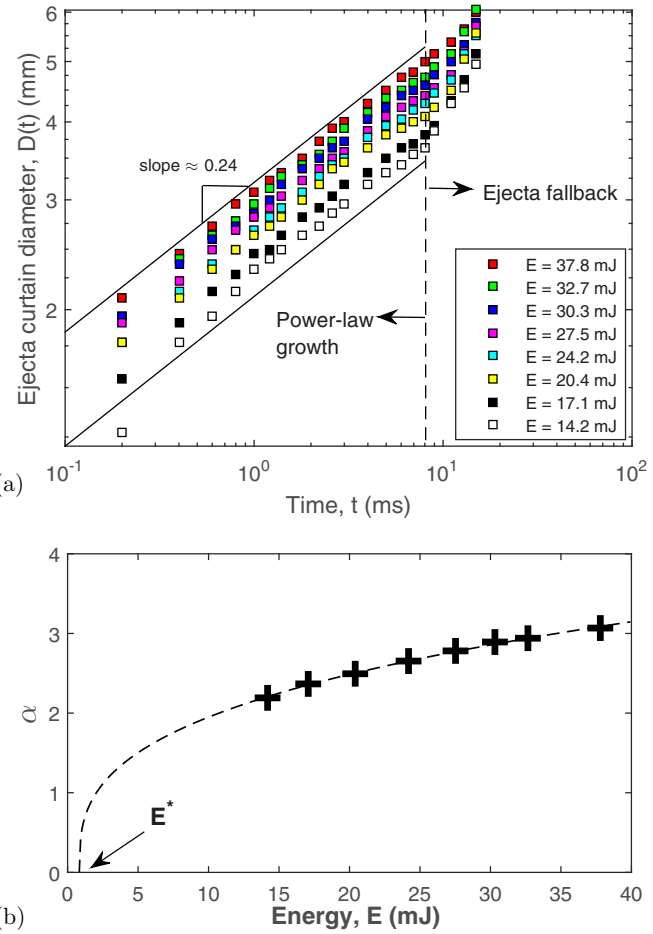


FIG. 4. (a) Temporal evolution of the ejecta curtain diameter for 31-$\mu$m glass beads For $t \lesssim 8$ ms, the ejecta growth is well described by a power law, $D = \alpha t^{0.24}$. (b) Dependence of the numerical prefactor on energy, $\alpha = 0.98(E - E^*)^{0.33}$ with $E^* = 0.83$ mJ.

comparison to solid surface ablation [34–36], where craters form due to rapid heating and evaporation, the laser energy required to form a crater herein ($10^{-3}$ J) is significantly lower because no material melting occurs and the loose noncohesive nature of the granular material means the shock wave can easily eject grains.

*Ejecta curtain evolution*. In the very first moments following the laser pulse, energy imparted by the pressure impulse is dissipated radially which results in individual grains ejected from the surface at high velocity, and also gives rise to an ejecta curtain which propagates radially away from the laser focal waist [see Fig. 2(a)]. The ejecta curtain typically starts to disintegrate and falls back to the granular surface around $t \approx 10$ ms. However, up to this time, we observe a consistent power-law growth with respect to time, $D = \alpha t^{0.24}$, as shown in Fig. 4(a).

The expansion rate of the ejecta curtain is virtually independent of the pulse energy since all the curves can be collapsed by a single power-law exponent, 0.24, while the numerical prefactor, $\alpha$, is found to exhibit a 1/3-power-law dependence on the laser energy, as shown in Fig. 4(b), meaning that the scaling for the overall ejecta curtain growth is $D \sim (E - E^*)^{1/3} t^{0.24}$. In this scaling, the exponent with respect to energy is different from that for the *final* crater

diameter, and is only valid over the early ejecta growth $t \leqslant 10$ ms, before the ejecta curtain disintegrates and falls back to the surface level. Although the time exponent of 0.24 is different from previous studies, we note that the recent laboratory-scale explosive cratering study [11] found a very similar power-law dependence for the ejecta curtain with $D \propto (m - m_0)^{1/3} t^{0.3}$, where $m$ was the mass of the explosive charge, thus implying the dynamics of laser-induced craters conform closely to explosive craters.

*Concluding remarks*. In conclusion, we have developed a technique for the production of millimetric granular craters by using a focused laser pulse. The focusing of light energy resulted in plasma formation and imparts a pressure impulse to the granular surface, which initiates the cratering process. Here we report small-scale craters in granular media, and confirm that power-law scalings for the crater size with respect to input energy are valid at these lengthscales, with empirical fits indicating that the minimum energy required to form a crater is on the order of $10^{-4}$ J. However, the exponents, varying between 0.31 and 0.43, appear to depend on the size and coarseness of the grains, and may be an indication that these factors are even more significant at the reduced energies and lengthscales herein, compared to large explosive craters. Assessing the temporal evolution of the ejecta curtain, we found a similar dependence on energy and time, i.e., $D \sim (E - E^*)^{1/3} t^{0.24}$, to that reported for explosive cratering.

While this work opens up the avenue for further research in small-scale cratering processes, our experiments here have also indicated that the specific granular characteristics such as particle size distribution and shape cannot be neglected when comparing energy scalings for cratering processes. Although the mechanisms and lengthscales are clearly distinct, the experiments herein using focused radiation may be related to the hypothesized sublimation mechanism for the formation of "pits" and "dark spots," on Mars and Pluto, respectively.

*Acknowledgments*. We thank Prof. Siggi Thoroddsen, as some of the early experiments were performed using the facilities of the high-speed fluids imaging laboratory at KAUST. We also thank the referees for comments that greatly improved the manuscript.

[1] H. J. Melosh, *Impact Cratering: A Geologic Process* (Oxford University Press, New York, 1989).
[2] *Impact Cratering: Processes and Products*, edited by G. R. Osinski and E. Pierazzo (Wiley-Blackwell, Hoboken, 2013).
[3] H. Katsuragi, *Physics of Soft Impact and Cratering* (Springer, Japan, 2016).
[4] A. J. Chabai, J. Geophys. Res. **70**, 5075 (1965).
[5] L. J. Vortman, J. Geophys. Res. **73**, 4621 (1968).
[6] K. A. Holsapple and R. M. Schmidt, J. Geophys. Res. B **85**, 7247 (1980).
[7] U.S. Army Engineer Waterways Experiment Station, Technical Report No. 2-547, 1961.
[8] F. E. Loranca-Ramos, J. L. Carrillo-Estrada, and F. Pacheco-Vázquez, Phys. Rev. Lett. **115**, 028001 (2015).
[9] H. H. Kieffer, P. R. Christensen, and T. N. Titus, Nature (London) **442**, 793 (2006).
[10] M. W. Telfer, E. J. R. Parteli, J. Radebaugh, R. A. Beyer, T. Bertrand, F. Forget, F. Nimmo, W. M. Grundy, J. M. Moore, S. Alan Stern, J. Spencer, T. R. Lauer, A. M. Earle, R. P. Binzel, H. A. Weaver, C. B. Olkin, L. A. Young, K. Ennico, and K. Runyon, Science **360**, 992 (2018).
[11] F. Pacheco-Vázquez, A. Tacumá, and J. O. Marston, Phys. Rev. E **96**, 032904 (2017).
[12] M. Gao, X. Liu, L. P. Vanin, T.-P. Sun, X. Cheng, and L. Gordillo, AICHE J. **64**, 2972 (2018).
[13] A. M. Walsh, K. E. Holloway, P. Habdas, and J. R. de Bruyn, Phys. Rev. Lett. **91**, 104301 (2003).
[14] S. J. de Vet and J. R. de Bruyn, Phys. Rev. E **76**, 041306 (2007).
[15] D. R. Dowling and T. R. Dowling, Am. J. Phys. **81**, 875 (2013).
[16] M. A. Ambroso, C. R. Santore, A. R. Abate, and D. J. Durian, Phys. Rev. E **71**, 051305 (2005).
[17] J. de Bruyn and A. M. Walsh, Can. J. Phys. **82**, 439 (2004).
[18] H. Katsuragi and D. J. Durian, Nat. Phys. **3**, 420 (2007).
[19] D. I. Goldman and P. Umbanhowar, Phys. Rev. E **77**, 021308 (2008).
[20] H. Katsuragi and D. J. Durian, Phys. Rev. E **87**, 052208 (2013).
[21] T. A. Brzinski, P. Mayor, and D. J. Durian, Phys. Rev. Lett. **111**, 168002 (2013).
[22] J. O. Marston and S. T. Thoroddsen, Powder Technol. **274**, 284 (2015).
[23] N. Kouraytem, S. T. Thoroddsen, and J. O. Marston, Phys. Rev. E **94**, 052902 (2016).
[24] S. T. Thoroddsen and A. Q. Shen, Phys. Fluids **13**, 4 (2001).
[25] D. Lohse, R. Rauhe, R. Bergmann, and D. van der Meer, Nature (London) **432**, 689 (2004).
[26] J. O. Marston, E.-Q. Li, and S. T. Thoroddsen, J. Fluid Mech. **704**, 5 (2012).
[27] W. K. Hartmann, Icarus **63**, 69 (1985).
[28] J. E. Colwell, S. Sture, M. Cintala, D. Durda, A. Hendrix, T. Goudie, D. Curtis, D. J. Ashcom, M. Kanter, T. Keohane, A. Lemos, M. Lupton, and M. Route, Icarus **195**, 908 (2008).
[29] D. E. Gault and J. A. Wedekind, *Impact and Explosion Cratering* (Pergamon, New York, 1977).
[30] H. Mizutani, S.-I. Kawakami, Y. Takagi, and M. Kumazawa, J. Geophys. Res. **88**, A835 (1983).
[31] K. A. Holsapple, Int. J. Impact Eng. **5**, 343 (1987).
[32] K. A. Holsapple, Annu. Rev. Earth. Planet. Sci. **21**, 333 (1993).
[33] K. R. Housen and K. A. Holsapple, Icarus **211**, 856 (2011).
[34] T. Desai, S. Batani, S. Rossetti, and G. Luchinni, *Conference Proceedings of the 32nd EPS Conference on Plasma Physics* (European Physical Society, Tarragona, Spain, 2005), Vol. 29C, D-1.001.
[35] E. Woryna, J. Badziak, P. Parys, R. Suchañska, J. Wolowski, J. Krása, L. Láska, M. Pfeifer, K. Rohlena, and J. Ullschmied, Nukleonika **47**, 147 (2002).
[36] V. N. Lednev, P. A. Sdvizhenskii, M. Ya. Grishin, V. A. Filichkina, A. N. Shchegolikhin, and S. M. Pershin, Appl. Opt. **57**, 11 (2018).
[37] P. Guo and X. Su, Can. Geotech. J. **44**, 579 (2007).
[38] F. Pacheco-Vázquez and J. C. Ruis-Suárez, Phys. Rev. Lett. **107**, 218001 (2011).
[39] J. S. Uehara, M. A. Ambroso, R. P. Ojha, and D. J. Durian, Phys. Rev. Lett. **90**, 194301 (2003).